ESRF	**Experiment title:** Effect of local gas flows and adapted intensity distributions on keyhole formation and melt pool dynamics in deep penetration laser beam welding	**Experiment number**: ME-1580
Beamline: ID19	**Date of experiment**: from: 16.09.2021 to: 28.09.2021	**Date of report**: 31.01.2022
Shifts: 12	**Local contact(s)**: Alexander Rack, Herwig Requardt, Yunhui Chen	*Received at ESRF:*

Names and affiliations of applicants (* indicates experimentalists):

Leander Schmidt[1,*], Klaus Schricker[1,*], Christian Diegel[1,*], Marc Seibold[1,*], Adrian Gottschall[1,*], Peter Hellwig[1,*], Fabian Fröhlich[1,*], Jean Pierre Bergmann[1], Peter Kallage[2,*], Falk Nagel[2,*], Oliver Forster[2,*], Oliver Kraus[2,*]

[1]: Technische Universität Ilmenau, Production Technology Group, Gustav-Kirchhoff-Platz 2, 98693 Ilmenau, Germany

[2]: COHERENT/Rofin-Sinar Laser GmbH, Application Lab, Berzeliusstraße 83, 22113 Hamburg, Germany

Report:

Laser beam welding with solid-state lasers leads to the formation of defects (e.g., spatters, pores) at relevant processing speeds (≥ 8 m/min). This phenomenon originated from the highly dynamic interaction of melt and metal vapor inside the keyhole [1]. The use of local gas flows and adapted laser intensities proved to be adequate to avoid spatter and pore formation [2], [3]. However, the underlying effects are not yet conclusively understood, which requires a spatial and time-dependent description of the keyhole and its stability.

Experiment:

In-situ high-speed synchrotron X-Ray imaging have been performed on beamline ID19 (Fig. 1a) to characterize spatial and time-dependent changes in keyhole geometry for laser beam welding of steel (high-alloy steel: X5CrNi18-10, galvanized steel: DX51D Z275), copper (Cu-ETP) and aluminium (wrought aluminium: EN AW 5754, cast aluminium: AlSi9MgMn) at welding speeds ≥ 8 m/min. A beam energy up to 60 keV and a beam size of 3 mm x 3 mm was used to pass 3-5 mm thick samples for image acquisition at frame rates up to 120,000 Hz. For the welding process, an adjustable ring mode (ARM) fiber laser with a wavelength of 1,070 nm and a maximum power of 8 kW was used to apply different concentric laser intensities, including conventional laser intensities (e.g. tophat intensity in Fig. 1b) or individual center/ring intensities (d_{center} = 75 mm, d_{ring} ≈ 200 µm, in Fig. 1c). For further tests, inert gas (argon, helium and nitrogen) was locally supplied to the keyhole aperture (Fig. 1d). Flow rate, angle of incidence and nozzle distance of the gas supply were varied.

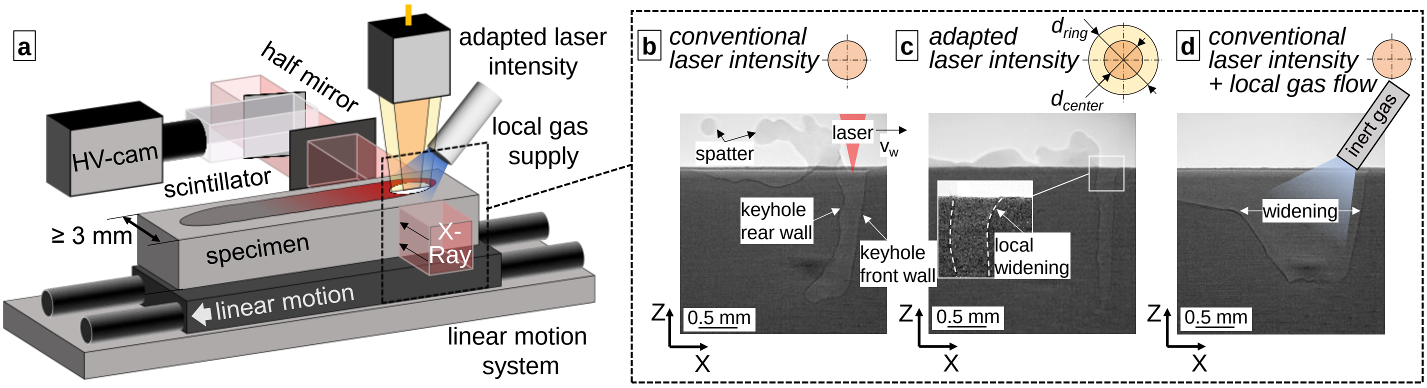

Figure 1: (a) Schematic of experimental setup, (b) - (d) in-situ synchrotron X-ray images of keyhole formation while using different laser intensities and a local gas flow at a welding speed of 12 m/min.

Experimental results:

The experimental setup allowed the image acquisition of keyhole formation for full penetration welding (Fig. 2a) and partial penetration welding (Fig. 1b-d, Fig. 2b-e) with high temporal resolution ($t_{res} \leq 0.05$ ms) and spatial resolution ($x_{res} \leq 2$ µm). In addition, it was also possible to visualize the keyhole surrounding melt pool for welding of aluminium (Fig. 2b-c) and copper (Fig. 2d), providing fundamental information about the solidification process. Due to the high temporal and spatial resolution, the formation of spatters and pores could be observed, correlated to keyhole fluctuations and linked to the effect of adapted laser intensities and local gas flows, which were primarily analyzed for welding of high-alloy steel. Depending on the set ratio of center and ring intensity, a change of the aspect ratio (keyhole depth to keyhole width) could be observed. An increasing ring intensity resulted in a widening of the upper-sided keyhole aperture (Fig. 1c). In contrast, the effect of the local gas flow was mainly related to changes in the formation and fluctuation amplitude of the keyhole rear wall (Fig. 1d). Depending on flow rate, the gas flow resulted in a stabilization of the keyhole rear wall followed by an extensive widening of the keyhole length. While these effects were observed for welding of high-alloy steel, the effect of local intensities was also investigated for welding of aluminum, copper and galvanized steels. For welding aluminum, an increased pore formation could be observed (Fig. 2b-c). In this context, pore formation of welded EN AW 5754 could be predominantly attributed to instabilities of the bottom-sided keyhole (keyhole collapse, Fig. 2b), whereas pores of welded AlSi9MgMn were mainly related to dissolved hydrogen of the base material (Fig. 2c). Welding of copper was mostly similar to welding of high-alloy steel (Fig. 2d). However, a melt pool elongation at the specimen top side was observed. For welding of galvanized steel sheets in overlap configuration, a significantly enlarged and unstable keyhole formation was found (Fig. 2e). Strong fluctuations of the keyhole rear wall resulted in a considerable formation of spatters due to zinc evaporation.

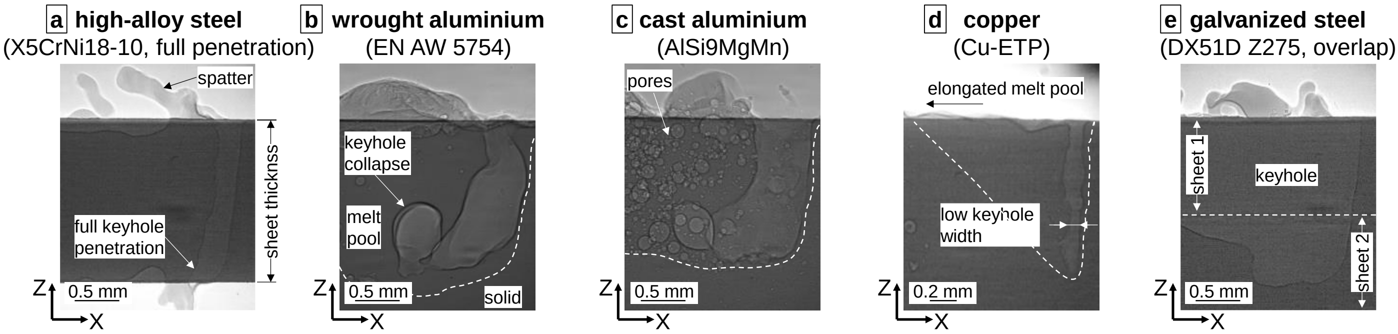

Figure 2: In-situ synchrotron X-ray images of keyhole formation while welding: a) high-alloy steel (full penetration), b) wrought aluminium, c) cast aluminiumm, d) copper and e) galvanized steel (overlap)

Outlook:

It is intended to quantify the effect of adapted laser intensities and local gas flows on keyhole formation. The use of image processing allows the extraction of relevant geometric keyhole parameters (e.g., inclination, width or length $l_{keyhole}$ in Fig. 3a). These data are used to analyze the dynamic behavior of the keyhole (e.g., keyhole length over time in Fig. 3b) to determine the oscillation amplitude and frequencies (e.g. by means of fast Fourier transformation algorithm (FFT) in Fig. 3c). The data will be used additionally for a 3D keyhole reconstruction to link intensity distributions of the laser beam to keyhole formation and dynamics based on raytracing.

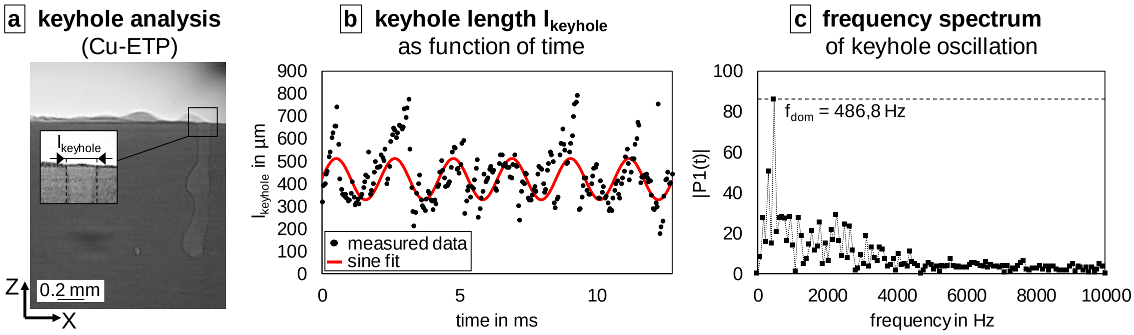

Figure 3: Analysis of keyhole fluctuations by: a-b) measuring keyhole length l_{keyole} as function of time and c) determination of the dominant keyhole oscillation frequency by means of fast Fourier transformation algorithm (FFT)

[1] - J. Volpp, "Keyhole stability during laser welding", Production Engineering, Vol. 11, p. 9–18 (2017). DOI: 10.1007/s11740-016-0705-4

[2] - L. Schmidt, K. Schricker, C. Junger, J.P. Bergmann, „Effect of local gas flow in full penetration laser beam welding with high welding speeds", Applied Sciences, Vol. 10, Nr. 5, p. 1867 (2020). DOI: 10.3390/app10051867

[3] - F. Nagel, L. Brömme, J.P. Bergmann, "Effects of two superimposed laser beams on spatter formation during laser welding of high alloyed steel", Journal of Laser Applications, Vol. 2, Nr. 31 022005 (2019). DOI: 10.2351/1.5040572